

Original Paper

Establishment of a Novel Fetal Ovine Heart Cell Line by Spontaneous Cell Fusion: Experimental Study

Khalid Suleiman, BVSc, MVSc, PhD; Mutaib Aljulidan, BSc; Gamaleldin Hussein, BVSc, MVSc, PhD; Habib Alkhalaf, BVSc, MVSc

Veterinary Vaccine Production Centre, Ministry of Environment, Water and Agriculture, Riyadh, Saudi Arabia

Corresponding Author:

Khalid Suleiman, BVSc, MVSc, PhD
Veterinary Vaccine Production Centre
Ministry of Environment, Water and Agriculture
PO Box 15831
Riyadh, 11454
Saudi Arabia
Phone: 966 501305563
Email: kmsuleiman67@gmail.com

Related Articles:

Preprint (JMIR Preprints): <https://preprints.jmir.org/preprint/53721>
Peer-Review Report by Hira Rafi (CU): <https://bio.jmirx.org/2024/1/e63336/>
Peer-Review Report by Arjama Mukherjee (DA): <https://bio.jmirx.org/2024/1/e62905/>
Authors' Response to Peer-Review Reports: <https://bio.jmirx.org/2024/1/e62911/>

Abstract

Background: The culture of immortal cell lines has become an indispensable tool in the field of modern biotechnology and has been used in the production of human and viral veterinary vaccines, therapeutic recombinant proteins, interferons, and monoclonal antibodies. Several approaches are used to immortalize cells in culture, such as transduction of cells with viral oncogenes, induced expression of telomerase reverse transcriptase, and spontaneous immortalization by serial passage of primary cell lines.

Objective: This study aimed to establish an immortal cell line by serial passage of fetal ovine heart cells that could be used to produce veterinary viral vaccines.

Methods: We serially passaged primary heart cells prepared from a fetal ovine heart till passage 140. We studied the events that led to the transformation and immortalization of the cell line under light and phase contrast microscopy. DNA samples of the cell line at passages 22 (before transformation) and 47 (after transformation) were genotyped according to single nucleotide polymorphisms (SNPs) using the OvineSNP50 BeadChip (Illumina). We sequenced the *cytochrome b* gene, control region, and *tRNA-Phe* and *12S rRNA* genes of the mitochondrial genome of the cell line at passages 26 and 59 by Sanger sequencing. The susceptibility of the cell line to sheep pox, Peste des petits ruminants (PPR), lumpy skin disease (LSD), Rift Valley fever (RVF), and camel pox viruses was investigated.

Results: We established a unique immortal cell line called fetal ovine heart–Saudi Arabia (FOH-SA) by serial passage of fetal ovine heart cells. We demonstrated that the transformation or immortalization of the cell line resulted from spontaneous cellular and nuclear fusion of 2 morphologically distinct cardiocytes at passage 29. Fused cells at passage 29 gave rise to progeny cells, which grew into multicellular filaments that persisted at passages 30, 31, and 32. Trypsinization of the filamentous multicellular growth at passage 32 gave an epithelial-type immortal heart cell line. SNP genotyping revealed 65% and 96% homozygosity in SNP genotypes of the cell line at passages 22 and 47, respectively. Partial sequencing of the mitochondrial genome of the cell line revealed mutational events in the control region and the *tRNA-Phe* and *12S rRNA* genes of the mitochondrial genome of passage 59 cells. The cell line was found to be permissive to sheep pox, PPR, LSD, RVF, and camel pox viruses.

Conclusions: We established an immortal cell line by serial passage of primary fetal ovine heart cells, which was permissive to many animal viruses. It could be used in animal virus isolation, vaccine production, and biotechnology. The study reported spontaneous cell fusion of cardiocytes as a method of cell immortalization. The findings of this study might help address the mystery of how the VERO cell line evolved.

(JMIRx Bio 2024;2:e53721) doi: [10.2196/53721](https://doi.org/10.2196/53721)

KEYWORDS

fetal ovine heart; cell line; serial passage; spontaneous cell fusion; SNP genotyping; mitochondrial genome sequencing

Introduction

Cell culture has become an indispensable tool in the field of modern biotechnology and has been used in the production of human and veterinary viral vaccines, therapeutic recombinant proteins, interferons (IFNs), and monoclonal antibodies [1-3]. Cell culture has also been used to study intracellular reactions through the creation of in vitro models for research and study the cytotoxicity of pharmaceuticals and bacterial toxins [4,5]. Recently, cell culture has emerged as a future candidate for the creation of cell-based meat intended for human consumption [6].

Primary cells obtained from mature or embryonic human and animal organs usually undergo a limited number of passages, after which they enter replicative senescence that is characterized by degenerative changes such as cell rounding, cell enlargement, decreased capacity to proliferate, and detachment from the monolayer [7,8]. At the molecular level, senescent cells show distinctive markers of senescence, such as increased expression of p53, p21, p16, and other cyclin-dependent kinase inhibitors like p27 and p15 [9-11].

In rare cases, some mammalian cells under continuous subculture escape replicative senescence and become spontaneously immortal, resulting in a continuous cell line [12,13]. The Madin-Darby bovine kidney (MDBK) and Madin-Darby ovine kidney (MDOK) cell lines were spontaneously immortalized by serial passage of cells from the renal tissues of *Bos taurus* and *Ovis aries*, respectively [14]. Recently, an ovine kidney cell line (FLK-N3) was also spontaneously established by serial passage of primary fetal lamb kidney cells from a fetus of a normal sheep [15]. The ubiquitous African green monkey cell line (VERO) was also spontaneously immortalized by serial passage of kidney cells of the African green monkey, and it has been deposited at the American Type Culture Collection (ATCC) at passage 113 to establish a bank for availability [16].

Over the last 35 years, numerous types of primary cell cultures have been used at the Veterinary Vaccine Production Centre in Riyadh, Saudi Arabia, to produce the sheep pox vaccine, which included ovine cells from the testicles, aortic endothelium, kidneys, and heart. Although the titers of the produced vaccine were satisfactory, the disadvantages associated with primary cultures, such as the risk of contamination, tediousness, inconsistency of cell characteristics, ethics of slaughtering animals and using organs to prepare cell cultures, and limited production capacity, created hurdles in the production wheel, especially in the face of increased demand in Saudi Arabia for this vaccine. Trials were required over the years to establish a continuous cell line to overcome the difficulties and disadvantages associated with the use of primary cultures in vaccine production. The objective of this study was to establish a continuous cell line by serial passage of the primary cells of the fetal ovine heart, which could be used in vaccine production.

Methods

Preparation of the Primary Cell Culture

In March 2013, a single pregnant ewe (*Harri* breed) was euthanized by exsanguination in accordance with the Implementing Regulations of the Law of Ethics of Research on Living Creatures of the NCBE (Article, 38) for the collection of fetal organs to prepare primary cell cultures necessary for the production of the sheep pox vaccine. The fetal heart was aseptically incised and used to prepare primary cell cultures. The heart muscle was cut to 0.5-1.0 cm, washed 3 times with 1× MEM (Minimum Essential Medium; Gibco), and digested under stirring with 0.25% trypsin 10 times for 30 minutes each time. After each cycle of digestion, the suspension was allowed to settle, and the supernatant was sieved through a sterile gauze and centrifuged at 1000 rpm for 5 minutes. The supernatant was then discarded, and the cell pellet was cultured in nonvented Roux flasks containing complete growth medium (CGM) consisting of 1× MEM (Gibco), 10% fetal bovine serum (FBS) (Gibco), 1% GlutaMAX (Gibco), and 50 µg/mL of gentamycin, and a pH of 7.2-7.4 was maintained with 5.6% sodium bicarbonate. The flasks were incubated at 37 °C in a normal incubator.

Established Cell Lines

Primary heart cell cultures obtained from extractions 1 to 8 were initially subcultured after 5 days and then after every 3 days, and this cell line was used for producing the sheep pox vaccine. A second cell line was established from heart extractions 9 and 10, which was first subcultured after 9 days and then serially passaged every 3 days. Samples of the second heart cell line at different passages were cryopreserved in Recovery Cell Culture Freezing Medium (Gibco) in liquid nitrogen at -80 °C. The second cell line derived from heart extractions 9 and 10 was named the fetal ovine heart–Saudi Arabia (FOH-SA) cell line.

Cell Morphology and Cell Line Transformation

Initially, the morphologies of the 2 cell lines were studied under an inverted bright field microscope (Olympus), and later, the morphology of the second cell line (extractions 9 and 10) was studied under an inverted phase contrast microscope (Olympus).

Cryopreserved cells at passages 20 to 27 were resuscitated and subcultured to study the transformation event under a phase contrast microscope (Olympus CKX53) with a camera (DP74, software CellSens). Cultured flasks were fixed with tape on the microscope stage in a walk-in normal incubator at 37 °C. We photographed fixed fields of passages 28, 29, 30, 32, and 33 every 3 hours for 24 hours and then every 24 hours for a total of 72 hours for each passage.

Growth Curve and Population Doubling Time

Three-day-old cultures of heart cell line passages 25 (before transformation) and 36 (after transformation) were seeded into 25-cm² nonvented Roux flasks at densities of 9144 cells/cm² and 6485 cells/cm², respectively. Flasks were incubated at 37

°C in a normal incubator, and cells were counted after day 1, 2, 4, 6, 8, and 10 using a Handheld Automated Cell Counter (Millipore). The growth curves of the 2 passages were constructed by plotting the log of growth against time, and the population doubling time was calculated using a standard formula [17].

Extended Incubation of the Cell Line at 37 °C

We observed that the monolayer of the cell line established after transformation (passage 33 and above) could be maintained at 37 °C for 3-4 weeks without showing signs of cell degeneration. To confirm this observation, we incubated passage 59 cultures at 37 °C for 6 months, with the growth medium being changed every 3 weeks. During storage, the monolayer was examined under an inverted microscope every week. At the end of the storage period, flasks were subcultured, and the sensitivity of the cells to sheep pox virus was determined.

DNA Preparation

DNA was extracted from a cell suspension containing approximately 5×10^5 cells/mL, using the MagNA Pure 96 DNA and Viral NA Small Volume Kit as instructed by the manufacturer (Roche). The DNA concentration was measured using the NanoDrop 2000 instrument (Thermo Scientific; 260 nm). DNA extracted from cells in passages 22, 26, 47, and 59 was aliquoted and stored at -80 °C.

Authentication and Mycoplasma Testing

A DNA sample at passage 22 was shipped to the European Collection of Authenticated Cell Cultures (ECACC), United Kingdom, for authentication of the cell line by mitochondrial DNA barcoding and detection of mycoplasma contamination. Currently, DNA barcoding is used to authenticate animal cell lines, and it uses the mitochondrial cytochrome c oxidase subunit I (*COXI*) gene as a barcode. The test is performed by polymerase chain reaction (PCR) amplification of a 617-bp segment of the mitochondrial *COXI* gene, followed by sequencing of the product and matching of the finding to a library of reference sequences [18].

Single Nucleotide Polymorphism Genotyping

We shipped aliquots of DNA samples of cell line passages 22 (before transformation) and 47 (after transformation) to the GeneSeek Laboratory of NEOGEN for single nucleotide polymorphism (SNP) genotyping using the OvineSNP50 BeadChip (Illumina). The OvineSNP50 BeadChip is a high-throughput microarray system developed by Illumina in collaboration with the International Sheep Genomics Consortium. The OvineSNP50 BeadChip map contains 54,241 ovine SNPs spanning all 26 autosomal chromosomes, the sex chromosomes, and the mitochondria. The bead chip uses the Infinium HD Assay to analyze DNA samples. Briefly, the Infinium Assay work-flow consists of an initial PCR-free amplification of DNA samples on day 1, followed by enzymatic fragmentation of the amplified samples, application of the fragmented samples to the bead chip, and incubation of the chip overnight for samples to hybridize on day 2. On day 3, hybridized samples are extended, fluorescently stained, and imaged by the iScan System (Illumina). The genotyping data

of the DNA samples at passages 22 and 47 generated by the Infinium Assay of the bead chip on the iScan System were analyzed using Illumina GenomeStudio version 2.0.2 and Illumina GenCall Version 7.0.0, with a low GenCall score cutoff equal to 0.050.

Partial Sequencing of the Cell Line Mitochondrial Genome

We sequenced 2 segments of the FOH-SA cell line mitochondrial genome at passages 26 (before transformation) and 59 (after transformation) using Sanger sequencing with the 3730xl DNA Analyzer and BigDye Terminator v3.1 Cycle Sequencing Kit (Applied Biosystems). Two pairs of primers designed by Meadows et al [19] from the complete ovine mitochondrial DNA [20] were used to amplify the segments. The first pair of primers (Cytb-F: 5'-GTCATCATCATTCTCACATGGAATC-3' and Cytb-R: 5'-CTCCTTCTCTGGTTTACAAGACCAG-3') was used for amplifying a 1272-bp region of the ovine mitochondrial *cytochrome b* gene (AF010406 positions 14078 to 15349). The second pair of primers (mtCR-F2: 5'-AACTGCTTGACCGTACATAGTA-3' and mtCR-R1: 5'-AGAAGGGTATAAAGCACCGCC-3') was used to amplify a 1246-bp fragment spanning part of the control region, the complete sequence of the *tRNA-Phe* gene, and the partial sequence of the *12S rRNA* coding RNA gene (AF010406 positions 15983 to 592).

Susceptibility of the Cell Line to Viruses

The sensitivity of the FOH-SA cell line to viruses was investigated by infecting it with several animal viral vaccine strains, including sheep pox virus (Romanian strain), Peste des petits ruminants (PPR) (Nigerian 75/1), Rift Valley fever (RVF) virus (Smithburn strain), lumpy skin disease (LSD) virus (Neethling strain), and a local attenuated isolate of the camel pox virus. Passage 36 cells were inoculated at a multiplicity of infection (MOI) of 0.01, and flasks were incubated at 37 °C. The monolayers were examined daily under an inverted microscope for the development of the cytopathic effect (CPE). Flasks were harvested when the CPE reached 90%-95%, and the tissue culture infective dose 50 (TCID₅₀) for each virus was determined by the Karber method [21].

Production of the Sheep Pox Vaccine

We have used the FOH-SA cell line since 2013 for producing sheep pox (Romania strain) and camel pox vaccines (local attenuated isolate). Cells were propagated in Roux (125, 175, and 225 cm²) and roller flasks (850 and 1700 cm²), and inoculation was performed with a MOI of 0.01. The viral suspensions were harvested when about 90% CPE was reached.

Cell Line Deposition at the ATCC for Patenting

Thirty cryotubes each containing more than 10^6 cells of the fetal heart cell line (FOH-SA) at passage 51 each were shipped on dry ice to the Foreign Animal Disease Diagnostic Laboratory (FADDL), United States Department of Agriculture (USDA) in Plum Island for safety testing of foot and mouth disease, PPR, sheep pox, and camel pox viruses as a prerequisite by the USDA prior to deposition at the ATCC. After passing safety testing,

25 cryotubes were shipped from the FADDL to the ATCC for deposition for the purpose of patenting under the Budapest Treaty on the International Recognition of the Deposit of Microorganisms for the Purposes of Patent Procedure.

Data Analysis

Images of DNA samples of the heart cell line at passages 22 and 47 generated by the iScan System in the Infinium Assay were analyzed with Illumina GenomeStudio software (GSGT version 2.0.2), which was used to call and report the genotypes of the SNP loci on the OvineSNP50 BeadChip. The number of SNPs called; the frequencies of A/A, A/B, and B/B SNP genotypes; the minor allele frequency (MAF); and the 50% GenCall Score for each sample were calculated using GenCall version 7.0.0 software [22]. Data of the partial sequencing of the mitochondrial genome were controlled for quality and trimmed by DNA Baser Assembler (v5.15.0; Heracle BioSoft), and pairwise sequence alignment (PSA) of mitochondrial DNA sequences was carried out with an EMBOSS Needle [23].

BLASTn was used to compare the sequences of *Cytb*, the control region, and the *tRNA-Phe* and *12S rRNA* genes of cell line passages 26 and 59 to the *Ovis aries* mitochondrial genome sequence database.

Ethical Considerations

A single pregnant ewe was used in the study, and it was handled in compliance with the Implementing Regulations of the Law of Ethics of Research on Living Creatures of the National Committee of Bioethics (NCBE) for the use of animals in experiments (Article, 38) [24]. The authors confirm that all the methods used in the study were approved by the Ministry of Environment, Water and Agriculture (MEWA). The authors also confirm that all the procedures and the experimental protocols were in accordance with the regulations and guidelines of the MEWA.

Results

Cell Line and Morphology

The first cell line obtained from heart extractions 1 to 8 consisted of fibroblast-like cells. The monolayer became confluent in 5 days, and cells were then subcultured every 3 days. This cell line was used for producing the sheep pox vaccine till it reached replication senescence at passage 11.

The second cell line derived from heart extractions 9 and 10 (FOH-SA) initially showed scanty growth; however, it was confluent after 9 days. The cell line revealed 2 cell morphologies (epithelial-like and fibroblast-like cells), and these prevailed to passage 28. Thereafter, the cells transformed in passages 29 through 32. Cells after passage 33 exhibited a constant epithelial morphology and were smaller in size compared to the mother cells. The FOH-SA cell line was successfully subcultured every 3 days till passage 140.

Transformation of the Ovine Heart Cells

Bright Field Microscopy

During serial passage of the heart cell line, a constant cell transformation event was documented under bright field

microscopy, which began at passage 27 by increased cell density of fibroblast-like cells. In passage 29, the 2 cell morphologies disappeared and were replaced by a filament monolayer. We documented that cells in passage 29 became connected with tubules detectable 3 hours after incubation, which led to cell fusion, and the nuclei of connected cells moved to a central location in the connecting tubule and became coupled to each other. Then, huge amounts of mitochondria from fused cells migrated and accumulated around the nuclei of fused cells. This was followed by the separation of fused cells into 2 progeny cells. After 72 hours of incubation in passage 29, a monolayer appeared in the form of filaments. The filamentous cell morphology was also documented in passages 30, 31, and 32. At passage 33, the cell line stopped growing in filaments, and thereafter, the morphology remained constant till the highest passage reached (passage 140).

The cell line that evolved after transformation consisted of 1 phenotype, had an increased proliferative potential, and showed a different CPE pattern to the sheep pox virus compared with the cells before transformation.

Phase Contrast Microscopy

Further details of the heart cell morphologies and the cell fusion process demonstrated by light microscopy were revealed by investigating the cell line under phase contrast microscopy. The fibroblast-like cells consistently produced long threads that were detectable 3 hours after incubation and remained demonstrable after 24 hours but became disintegrated and could not be detected after 48 hours of incubation (Figure 1). In passage 28, the 2 cell phenotypes appeared as islets of epithelial-like cells surrounded by fibroblast-like cells (Figure 2).

In passage 29, instead of growing and multiplying, the fibroblast-like cells projected their threads that reached the epithelial-like cells, resulting in the establishment of connections that developed into tubules connecting the 2 cell types. When the 2 cell phenotypes existed close to each other, they directly fused, and such fusion points could be detected 3 hours after incubation of passage 29 cells. The nuclei of the fused cells appeared coupled together with huge amounts of mitochondria accumulating around them (Figure 3A-D).

When mitochondrial recruitment was complete, the 2 nuclei became confined and compressed in part of the cytosol of the 2 fused cells and became completely delineated from the rest of the cytosol of the fused cells. This was followed by a reaction in which complete fusion of the 2 nuclei was documented, characterized by the disappearance of the nucleoli and increased brightening of the fused nuclei. We described this event as a “nuclear fusion reaction.” When the nuclear fusion reaction was complete, the fused nuclei amalgamated with part of the cytosol of the fused cells to create the body of evolving progeny cells that eventually separated into 2 daughter cells (Figure 4A-F).

The first progeny cells from spontaneous cell fusion came into existence about 9 hours after incubation. It was observed that horizontally coupled nuclei gave rise to nascent cells with epithelial cell-like morphology, while fibroblast-like progeny cells evolved from the vertically coupled nuclei (Figure 5A and B).

The process of cell fusion and the appearance of new progeny cells continued in passage 29 cells, and 24 hours after incubation, approximately 95% of the cell population had completed spontaneous cell fusion and produced progeny cells (Figure 6A). Each progeny cell resulting from cell fusion in passage 29 then grew and multiplied, and 72 hours after incubation, progeny cells appeared as long multicellular filaments (Figure 6B-D). Trypsinization of the 72-hour culture at passage 29 resulted in single cells (Figure 7), and these cells when cultured (passage 30) grew into multicellular filaments. The pattern of multicellular filamentous growth was also documented in passages 31 and 32. Finally, when the passage 32 cells grown for 72 hours were trypsinized and cultured (passage 33), the progeny cells stopped growing into multicellular filaments, and thereafter, the cell morphology remained constant till the highest passage reached (passage 140) (Figure 8).

Although the final cell line had an epithelial-like morphology, there were 2 morphological types of cells (fibroblast-like cells and epithelial-like cells) similar in morphology to the parent cells, but this distinction could only be detected during the first

3-5 hours of culture incubation, after which the cell line appeared to have only 1 cell morphology.

When we examined many fields of the passage 30 culture, points of cell fusion surrounded by a matrix of second-generation growing progeny cells were detected. These fused cells represented cells that had failed to fuse in passage 29 due to physical distancing. These cells possessed exceptionally large nuclei with prominent nucleoli. The events following cell fusion proceeded as described before. Moreover, the nuclear fusion was preceded by the clear disintegration of the nuclear membranes of the fusing nuclei and obvious blending of the genetic material of the 2 nuclei. In addition, the nuclear reaction was accompanied by a very brilliant glow indicative of the high energy provided by the mitochondria to complete the fusion reaction (Figure 9A-F). A schematic summary of the spontaneous cell fusion process is shown in Figure 10.

In general, during the study of spontaneous cell fusion between the 2 heart cell phenotypes, we observed that the cell fusion process was photosensitive, and prolonged exposure of a fixed field during documentation by photography resulted in delay and sometimes abortion of the cell fusion process in the specific field under examination.

Figure 1. Morphology of the heart cell line at passage 22. (A) A 3-hour culture showing fibroblast-like cells developing long threads and epithelial-like cells appearing rounded in shape. (B) The same culture in A after 48 hours of incubation showing both cell types with fibroblast-like cells without threads. Imaging was performed using a phase contrast microscope ($\times 200$).

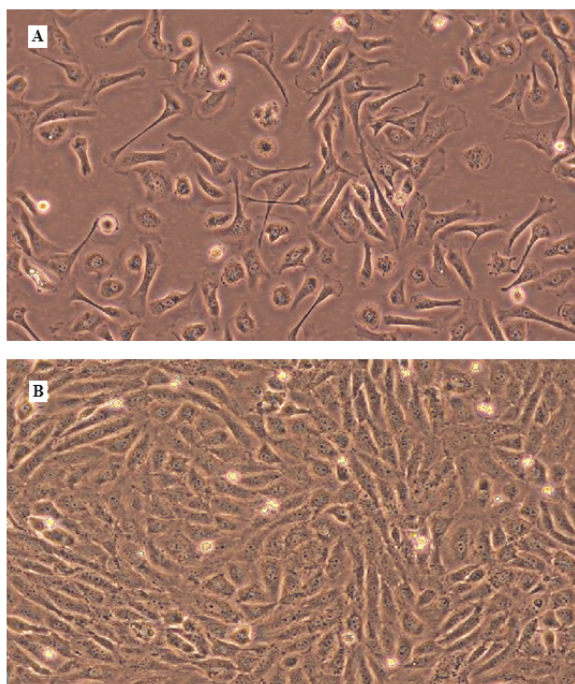


Figure 2. Morphology of the heart cell line. (A) Passage 26 culture showing fibroblast-like cells in a bundle growing diagonal to the field and epithelial-like cells above and below the bundle. (B) Passage 28 culture showing epithelial-like cells surrounded by bundles of fibroblast-like cells. Imaging was performed using a phase contrast microscope ($\times 200$).

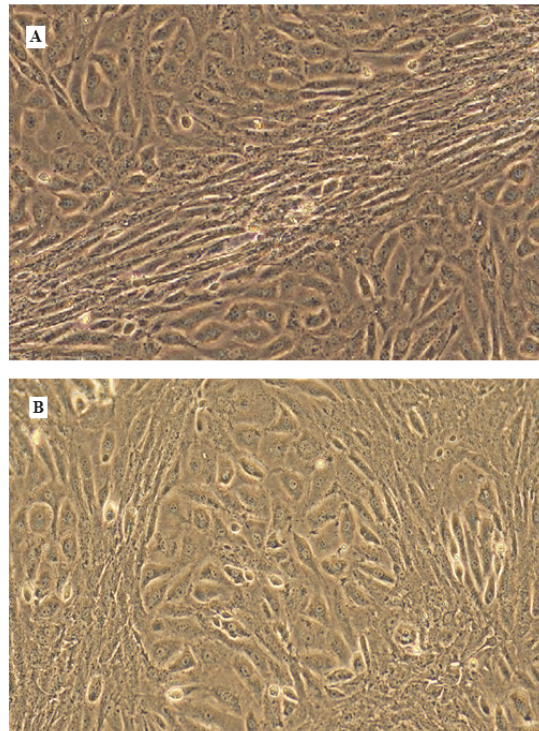


Figure 3. A 3-hour culture of the heart cell line at passage 29. (A, B) Heart cell phenotypes connected by tubules and points of spontaneous cell fusion with aggregated mitochondria around coupled nuclei of fused cells. (C, D) Two points of cell fusion after 3 and 6 hours of incubation. Imaging was performed using a phase contrast microscope ($\times 200$).

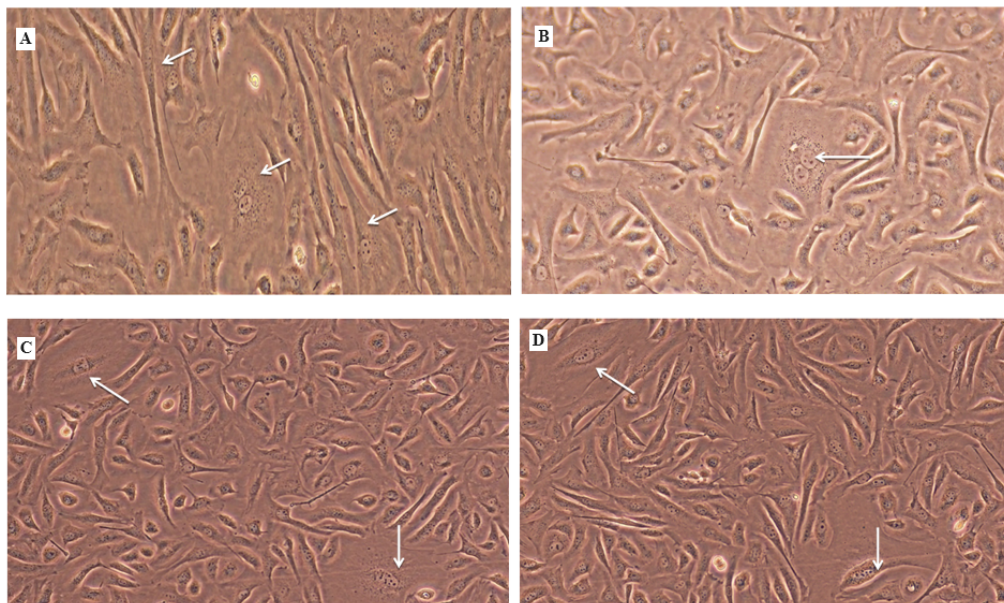


Figure 4. Stepwise progression of the spontaneous cell fusion process in passage 29 heart cells. (A) A 3-hour postincubation culture showing the point of cell fusion and coupling of nuclei. (B) A 7-hour postincubation culture showing the coupled nuclei becoming demarcated with part of the cytosol. (C) An 8-hour postincubation culture showing the nuclear fusion reaction. (D) An 11-hour postincubation culture showing the nucleoli of the 2 progeny cells. (E) An 18-hour postincubation culture showing the nuclei of the progeny cells becoming prominent. (F) A 21-hour postincubation culture showing the 2 nuclei of the progeny cells settling beside each other. Imaging was performed using a phase contrast microscope ($\times 200$).

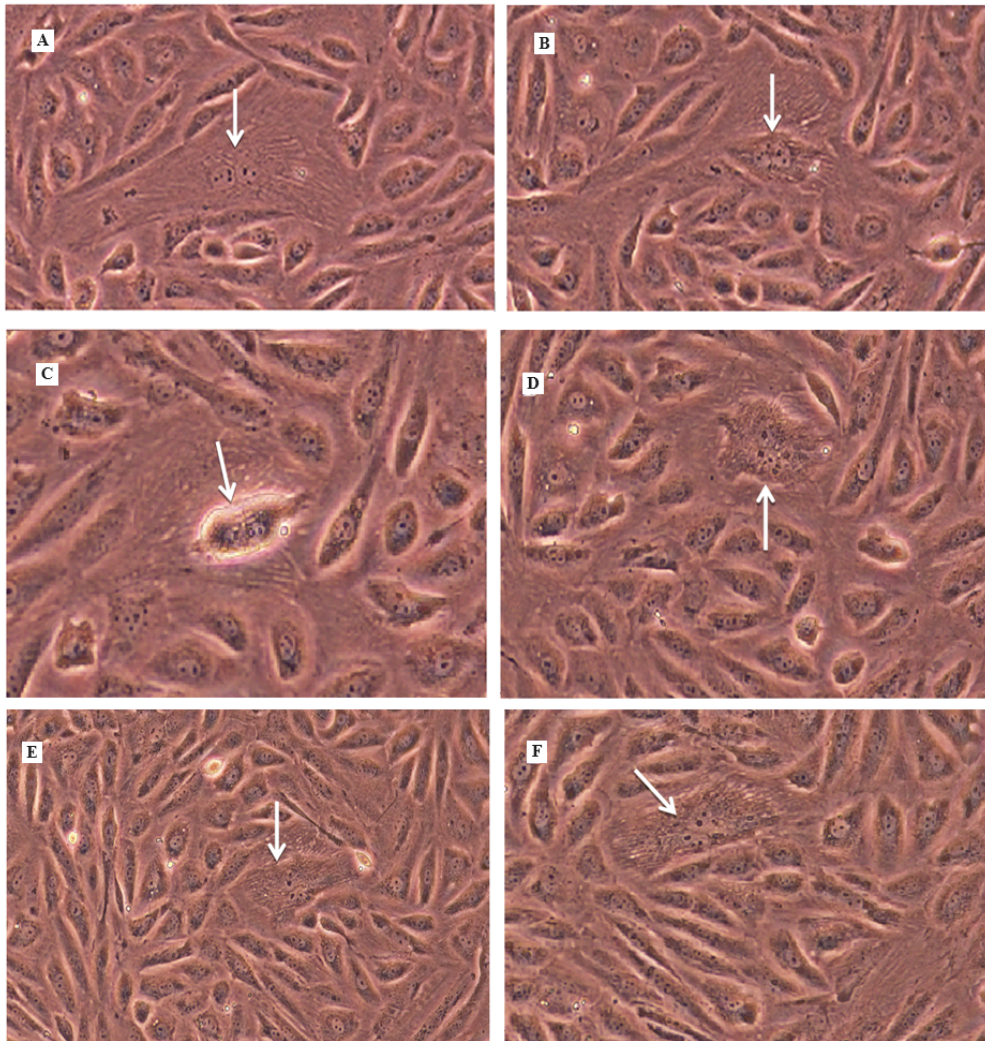


Figure 5. Heart cell line at passage 29. (A) A 6-hour postincubation culture showing 2 points of cell fusion (white arrows). (B) A 9-hour postincubation culture (the same field) showing 2 fibroblast-like cells and 2 epithelial-like cells that developed from the 2 fusion points in A (white arrows) and showing 2 new cell fusion points in the field (black arrows). Imaging was performed using a phase contrast microscope.

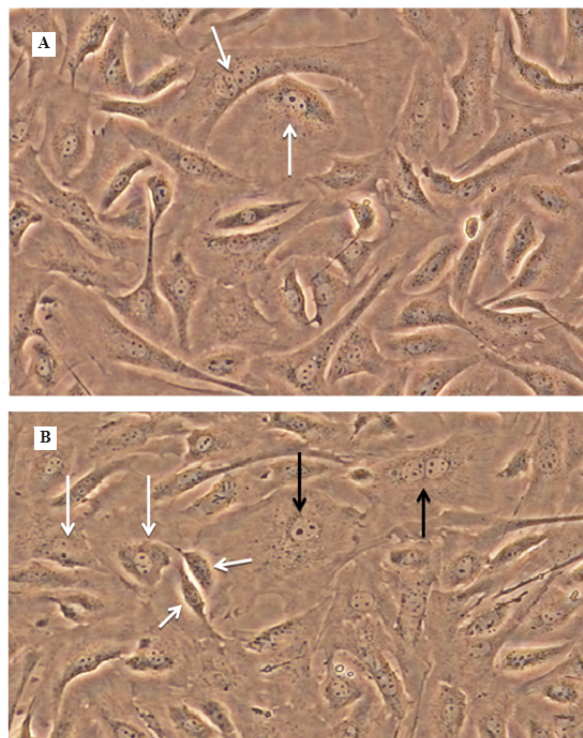


Figure 6. Growth of the progeny cells that developed after spontaneous cell fusion in passage 29 (same culture as in Figure 5). (A) Progeny cells 24 hours after incubation. (B) Growing progeny cells 36 hours after incubation. (C) Cells 48 hours after incubation. (D) The progeny cells have grown into long multicellular filaments 72 hours after incubation. Imaging was performed using a phase contrast microscope ($\times 200$).

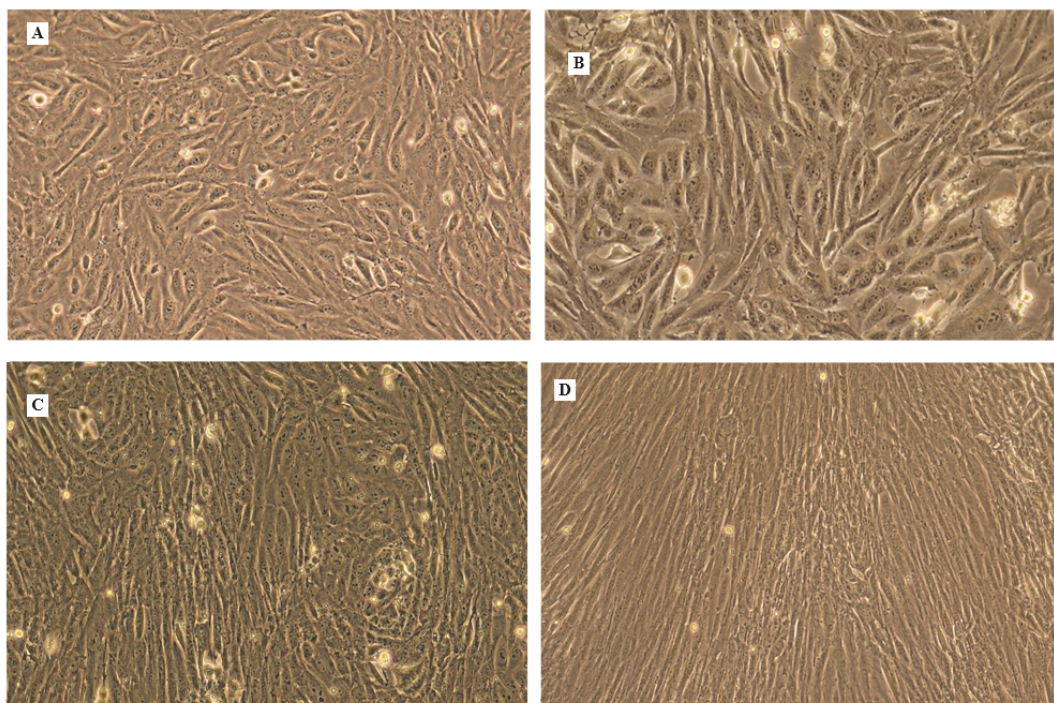


Figure 7. The heart cell line at passage 30 (3 hours after incubation). This is the first generation of cells after spontaneous cell fusion in passage 29, which resulted after trypsinization of the 72-hour multicellular filamentous growth in passage 29. Imaging was performed using a bright field microscope ($\times 200$).

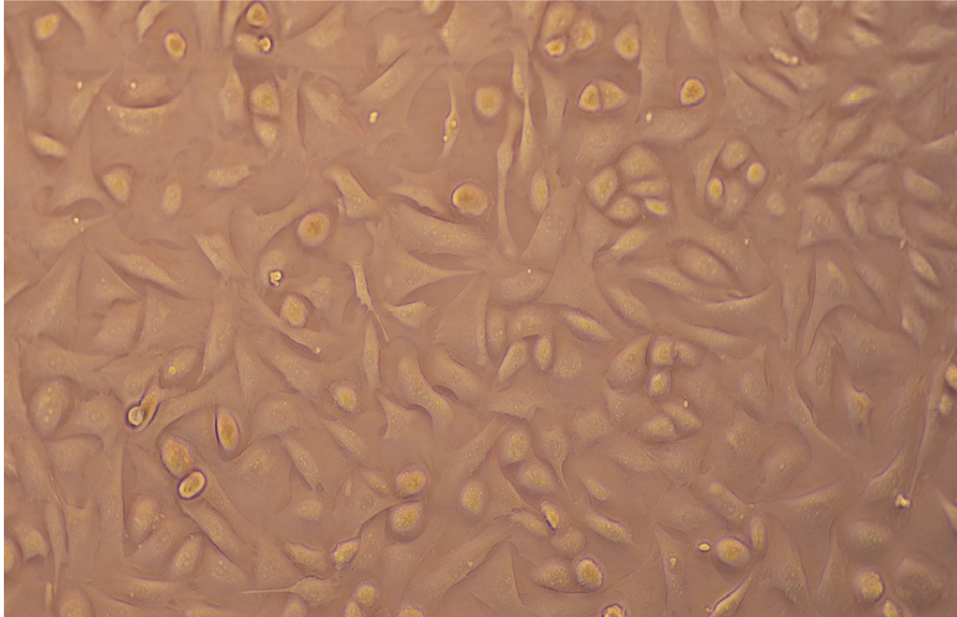


Figure 8. Morphology of the heart cell line at passage 33 after 48 hours of incubation. This morphology remained constant in the subsequent subcultures till passage 140. Imaging was performed using a phase contrast microscope ($\times 100$).

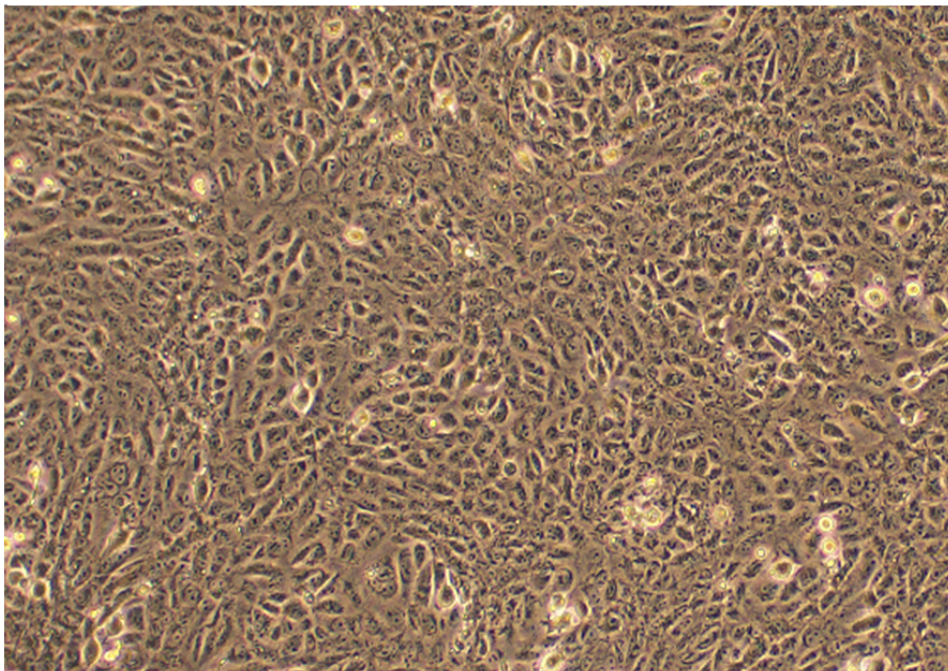


Figure 9. Point of spontaneous cell fusion in passage 30. (A) A 24-hour postincubation culture showing cell fusion and coupling of nuclei with accumulation of mitochondria around them. (B) A 46-hour postincubation culture showing disintegration of the nuclear membranes of the 2 nuclei and rearrangement of their genetic material. (C) A 48-hour postincubation culture showing complete mix up of the genetic material of the 2 cells. (D) A 49-hour postincubation culture showing a nuclear fusion reaction with massive liberation of energy (burning of the genetic material). (E) A 50-hour postincubation culture showing cooling down of the nuclear fusion reaction and reappearance of the genetic material in the developing progeny cells. (F) The 2 nuclei separate at the end of the nuclear fusion reaction (photographed from a different culture). Imaging was performed using a phase contrast microscope ($\times 200$).

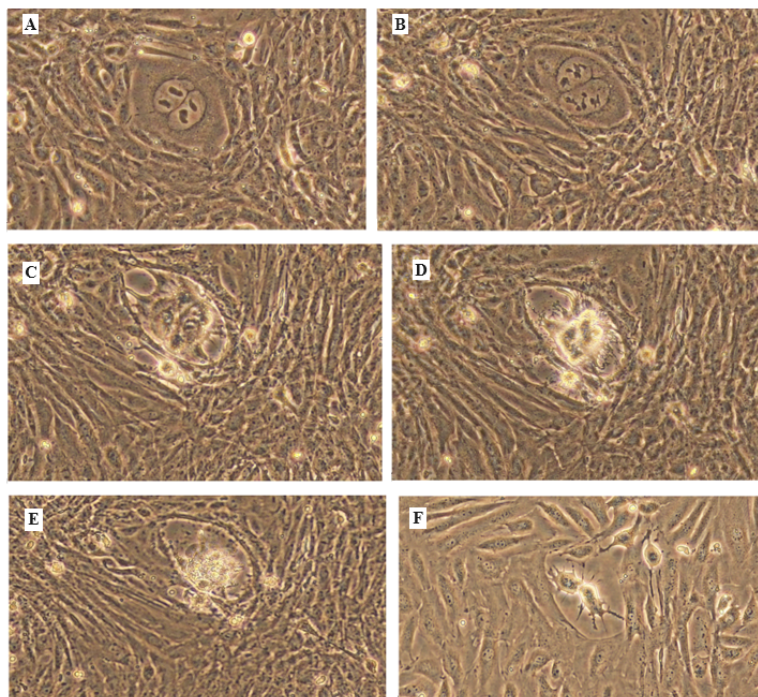
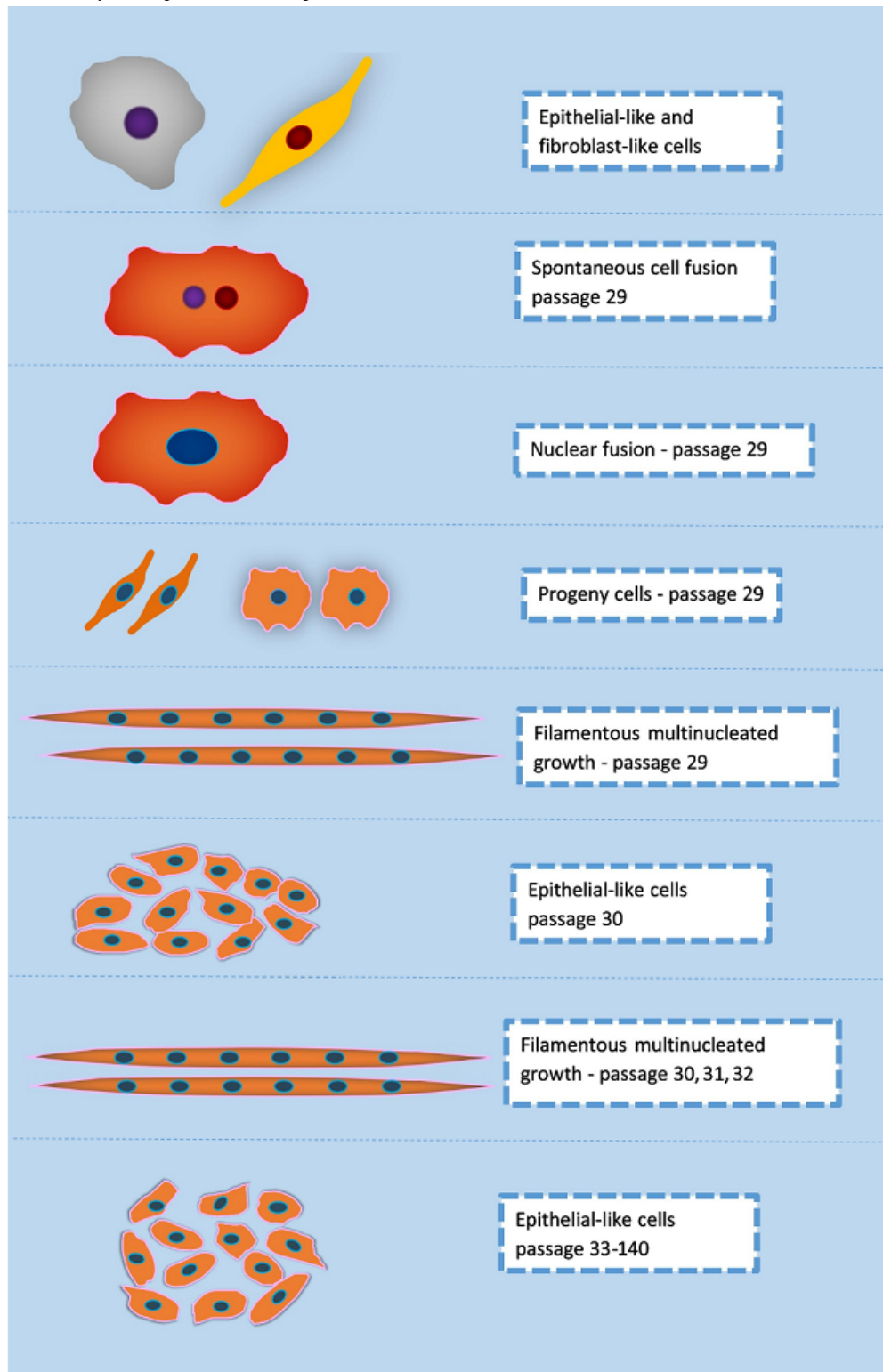


Figure 10. Schematic summary of the phenomenon of spontaneous cell fusion between fetal ovine heart cells in vitro.



Growth Curve and Population Doubling Time

A characteristic growth curve of cells after transformation was established using a 3-day-old culture at passage 36. The curve showed no lag phase. The highest growth rate was in the first 24 hours, and the log phase continued for 10 days. Transformed cells had a population doubling time of 14.5 hours compared to 25.8 hours for cells before transformation. The growth curve

of the heart cell line at passage 36 is shown in Figure S1 in [Multimedia Appendix 1](#).

Extended Incubation at 37 °C

The FOH-SA cell line was successfully subcultured after 6 months of storage at 37 °C; however, trypsinization of the culture required 30 minutes rather than the usual 5 minutes, and the whole monolayer came out as 1 sheet, which was broken down after rigorous shaking and pipetting. During the storage

period, the cell monolayer showed no signs of degeneration; however, numerous islets could be detected in the monolayer, in which the cells again acquired the ability to multiply in multicellular filaments, similar to the filamentous cell morphology reported in the transitional passages 29-32 (Figure S2 in [Multimedia Appendix 1](#)). After storage, the cells remained sensitive to sheep pox virus, and the CPE pattern remained similar to that of the original cells.

Cell Line Authentication

Authentication of the ovine heart cell line at the ECACC revealed that the mitochondrial DNA barcode of passage 22 cells matched 99% to *Ovis aries* (top 100 results on BLAST). The result of mycoplasma PCR analysis at the ECACC documented that the heart cell line was free of mycoplasma.

SNP Genotyping

Of 54,241 SNPs on the bead chip, 50,653 (93.4%) in the DNA sample of passage 22 cells were called. The genotype frequencies of the SNP alleles in the sample were 0.65 homozygous and 0.35 heterozygous.

In the DNA sample of passage 47 cells, 45,774 SNPs were called, which represented 84.4% of the total number of SNPs on the bead chip. The genotype frequencies of the alleles in the sample were 0.96 homozygous and 0.04 heterozygous.

The total number of SNPs called, the genotypes of the SNPs, the minor allele frequencies, and the 50% GenCall Score of each of the DNA samples are shown in [Table 1](#).

A total of 4879 SNPs called in passage 22 were not called in passage 47. The no-call SNPs were distributed throughout the chromosomes. The highest numbers were reported in chromosomes 3, 2, 1, 5, and 9. The no-call SNPs occurred singly and in succession of 2, 3, 4, and 5 SNPs. The genes spanning the 3, 4, and 5 successive no-call SNPs were identified by inserting the location of each set of SNPs in ENSEMBL (Table S1 in [Multimedia Appendix 1](#)).

The genetic conversion was also documented in the mitochondrial SNPs *mt.7729*, *CytB_1505.1*, and *CytB_1745.1*. The alleles of these SNPs were 100% BB homozygous in passage 22 cells (before transformation) and became 67% AA and 33% BB homozygous in passage 47 cells (after transformation).

The single SNP in the Y chromosome (*oY1.1*; index 37199 in the SNP map) was not called in the cell line either before transformation or after transformation. Accordingly, we concluded that the cell line was established from a female ovine fetus as the sex of the fetus was not checked during the preparation of the primary cultures.

Table 1. OvineSNP50 BeadChip genotyping of the fetal ovine heart cell line.

DNA sample	SNPs ^a called ^b , n	A/A frequency ^c	A/B frequency ^d	B/B frequency ^e	MAF ^f	50% GenCall Score
Passage 22 ^g	50,653	0.30	0.35	0.35	0.48	0.903
Passage 47 ^h	45,774	0.95	0.04	0.01	0.03	0.875

^aSNP: single nucleotide polymorphism.

^bSNPs in each sample with a GenCall Score above the no-call threshold.

^cThe number of A/A SNP genotype calls divided by the total number of calls.

^dThe number of A/B SNP genotype calls divided by the total number of calls.

^eThe number of B/B SNP genotype calls divided by the total number of calls.

^fMAF: minor allele frequency.

^gCell line before cell fusion.

^hCell line after cell fusion.

Sequencing of the Cytochrome b Gene

Sequencing of the *Cytb* gene of the heart cell line at passages 26 and 59 produced sequences of 1078 bp and 1061 bp, respectively. After quality control and trimming, the length of the *Cytb* gene was 834 bp for passage 26 cells and 858 bp for passage 59 cells. BLASTn analysis of *Cytb* of passage 26 cells revealed 99.28% identity to 100 BLAST hits of the *Ovis aries* complete mitogenome. Pairwise alignment of the partial sequences of the *Cytb* gene of the 2 cell passages showed 93.8% similarity with 6.2% gaps (Figure S3 in [Multimedia Appendix 1](#)). BLASTn analysis of the partial sequence of the *Cytb* gene of passage 59 cells showed 99.88% identity to the top 100 BLAST hits of the *Ovis aries* mitogenome, and this sequence was deposited in the GenBank database (GenBank accession: ON811684).

Sequencing of the Control Region and the tRNA-Phe and 12S rRNA Genes

The partial sequencing of the control region and the *tRNA-Phe* and *12S rRNA* genes of the heart cell line mitogenome resulted in a sequence of 1088 bp for passage 26 cells and 1083 bp for passage 59 cells. However, after trimming and quality control, the size of the sequences was 828 bp for passage 26 cells and only 305 bp for passage 59 cells. The 100 top BLAST hits for the passage 26 partial sequence revealed 98.67%-99.88% identity to the *Ovis aries* control region and the *tRNA-Phe* and *12S rRNA* mitogenome genes. PSA of the 828 bp sequence of passage 26 cells and 305 bp sequence of passage 59 cells revealed only 25.6% similarity with 67.9% gaps (Figure S4 in [Multimedia Appendix 1](#)).

Susceptibility to Viruses

The FOH-SA cell line was found to be highly susceptible and permissive to all tested viruses. The CPE of the RVF virus was detected within 48 hours in the form of cell elongation, syncytia formation, and monolayer disruption. The RVF virus suspension was harvested after 4 days, and the TCID₅₀ was 10^{7.1}/mL. The CPE of the PPR virus was detected within 72 hours in the form of cell rounding, syncytia formation, and adherence of the monolayer to the surface. The virus was harvested after 5 days, and the TCID₅₀ of the harvest reached 10^{7.3}/mL. The LSD virus showed a CPE similar to that of the PPR virus; however, it dismantled the monolayer sheet. The virus was harvested after 5 days, and the TCID₅₀ of the harvest was 10^{7.5}/mL. The CPE of the camel pox virus was detected after 48 hours in the form of cell rounding, large syncytia, and monolayer detachment. After 3 days, the TCID₅₀ of the harvest was 10^{7.5}/mL. The CPE of the sheep pox virus was detected after 48 hours. The virus was harvested after 5 days, and the TCID₅₀ of the harvest was 10^{7.5}/mL. The CPEs of the sheep pox, camel pox, and PPR viruses are shown in Figure S5 in [Multimedia Appendix 1](#).

Production of the Sheep Pox Vaccine

The cell line was used since its establishment in 2013 mainly for producing sheep pox and camel pox vaccines. Over the years, production was carried out in cell line passages ranging from 38 to 115, and satisfactory viral suspensions with TCID₅₀ values of 10^{7.1}/mL to 10^{7.5}/mL were obtained for both vaccines.

ATCC Cell Line Deposition

The FOH-SA cell line passed all the safety tests performed by the FADDL, including freedom from FMD, PPR, and sheep and camel pox viruses. Thereafter, it was shipped to the ATCC where it was processed in accordance with the Budapest Treaty, and the relevant international Budapest Treaty forms were issued. The cell line was deposited under the patent accession number PTA-125751.

Discussion

Establishment of a Fetal Ovine Heart Cell Line

This study describes the establishment of a continuous cell line by serial passage of fetal ovine heart cells. The cell line consistently transforms at passage 29 because of spontaneous cell fusion between 2 distinct heart cell types. The progeny cells resulting from the fusion process grow in the form of multicellular filaments in passages 29, 30, 31, and 32, after which the cell line shows an epithelial morphology.

Comparative SNP genotyping of the cell line before and after cell fusion revealed large-scale genetic conversion resulting in high homozygosity in the progeny cells. Partial sequencing of the mitochondrial genome of the cell line showed mutational events in the control region and the *tRNA-Phe* and *12S rRNA* genes of the mitochondrial genome in the progeny cells. The cell line was permissive to sheep pox, PPR, LSD, RVF, and camel pox viruses.

Spontaneous Cell Fusion

Spontaneous immortalization of mammalian cells is a rare event where spontaneous upregulation of the telomerase reverse transcriptase enzyme or low expression of p15, p16, or Rb allows cells to escape replication senescence and become immortal [25-27].

Although numerous animal cell lines have been spontaneously immortalized by serial passage, the exact mechanisms causing cell immortalization remain unexplained. For instance, the mechanisms that led to the establishment of the VERO cell line, which was derived from the serial passage of normal kidney cells, remain unexplained, although the cell line was established decades ago.

The transformation event documented in this study passed undetected during the initial serial passaging to establish an immortal heart cell line; however, the sufficient amount of cells stored before transformation allowed us to repeatedly derive the cells through passage 29, which enabled us to precisely observe and explain the events that led to cell transformation. If this approach was not followed, the transformation event reported in this study would have remained unexplained. Ogle et al [28] stated that the origin of a cell as the product of a fusion event can be difficult or impossible to deduce.

In this study, we established an immortal fetal ovine heart cell line through serial passage and we described the unprecedented method of cell immortalization in which 2 heart cell phenotypes spontaneously fused and then segregated into 2 progeny cells that had a different morphology and a smaller size compared with the parent cells, had an increased proliferation potential, exhibited a transitional phase of filamentous growth, showed immortality, and were susceptible to numerous animal viruses.

Fusion of cells of the same type or different types and fusion of their nuclei were found to occur *in vivo*, yielding hybrid cells known as heterokaryons (multinuclear) or sinkaryons (mononuclear). In sinkaryons, resorting and recombination of chromosomal DNA could occur, and the mononuclear daughter cells resulting from the hybrid cells have been found to express all the genetic material of the parental cells [29,30].

In this study, spontaneous cell fusion between the fibroblast-like and epithelial-like heart cell phenotypes was repeatedly documented at passage 29 (cells were subcultured every 3-4 days) and was not detected at any earlier passage. This could mean that these cell types became mature and competent for fusion at this specific age (29 passages), possibly by expressing the necessary cell fusion proteins and having mature mitochondria capable of providing the energy necessary for the nuclear fusion reaction. Recent work has identified fusion proteins (fusogens) as indispensable molecules in the fusion process between mammalian myoblast cells [29,31]. Similar fusogens might have mediated the fusion of the heart cells documented in this study.

In this study, we observed 2 types of spontaneous cell fusions. Adjacent fusion occurred when the 2 phenotypes existed in the neighborhood and was detected within 3-5 hours after incubation of passage 29 cells. The second type of cell fusion occurred when the cell types were distantly placed from each other. In

this type, the fibroblast-like cells protruded projections reaching the epithelial-like cells, and eventually, a tubule was established connecting the 2 cells. Shortly after cell fusion, coupling of the nuclei of the fused cells occurred, which triggered the migration of the mitochondrial population of the 2 cells to the site of nuclear coupling. The force driving the 2 nuclei to a coupling site at the tubular junction between the 2 cells could not be explained in this study. The mitochondrial migration was found to be crucial for initiating the nuclear fusion process, and it was only triggered when all the mitochondria of the fusing cells accumulated at the site of the coupled nuclei.

Cell fusion in vitro was induced by treating human lymphocytes with polyethylene glycol [32]. A second approach for cell fusion in vitro, known as electrofusion, was experimented by applying electric impulses to cells suspended in an appropriate electrofusion buffer [33,34]. Both methods resulted in hybrid cells with 2 or 3 nuclei; however, no nuclear fusion between the nuclei of the hybrid cells was demonstrated in these studies. Hence, the spontaneous cell fusion and nuclear fusion described in this study are novel unprecedented phenomena in cell biology.

In this study, the spontaneous cell fusion between the 2 heart cell phenotypes at passage 29 could be viewed as a type of cell mating (sexual reproduction), which was followed by a form of cell multiplication that could be considered asexual reproduction, in which each progeny cell grew into multiple cells that remained connected to each other and formed filaments. This pattern of cell multiplication was documented in the transitional passages 29, 30, 31, and 32 and could be described as resembling septate hyphae resulting from asexual reproduction in fungi. An early report described in vitro mating between 2 clonal lines of mouse fibroblasts that resulted in hybrid cells with evidence of segregation after mating; however, research in cell mating was discontinued and no other reports are available [35].

SNP Genotyping

The OvineSNP50 BeadChip has been used in many applications, including genome-wide selection, comparative genetic studies, and breed characterization for evaluating biodiversity [36-38]. It was validated by Illumina for genotyping of more than 3000 samples from diverse *Ovis aries* domestic and wild breeds [19]. In this study, we used the bead chip to compare the genotype of the cell line before and after cell fusion. SNP genotyping of DNA of the heart cell line at passage 22 revealed 50,653 polymorphic loci representing 93.4% of the SNPs on the bead chip, which was higher than the highest number of polymorphic loci reported in all domestic ovine breeds (*Rasa aragonesa* breed of sheep exhibited the highest polymorphic loci of 48,676) during the validation of the bead chip by Illumina. The *Harri* sheep breed, the sheep breed from which the heart cell line was established, was not included in the buildup of the bead chip.

SNP genotyping of passage 47 cells showed 0.95 A/A and 0.01 B/B SNP genotype frequencies compared to 0.30 A/A and 0.35 B/B genotype frequencies in the DNA samples at passage 22, while the frequencies for heterozygosity were 0.35 and 0.04 for passages 22 and 47, respectively. These results indicate that the spontaneous cell fusion resulted in large-scale genetic conversion in progeny cells involving about 65% of the alleles,

resulting in 96% homozygosity. Osada et al [39] identified the single nucleotide variants of the African green monkey (*Chlorocebus sabaues*) cell line (VERO) nuclear genome and reported 87.7% homozygosity. They attributed the high homozygosity to the evolutionary divergence between the genus *Macaca* and *Chlorocebus* from approximately 8-12 million years ago.

The MAF of the heart cell line before cell fusion was 0.48 and after cell fusion was 0.03. The MAF of 0.03 for the FOH-SA cell line after cell fusion indicated that the FOH-SA cell line was a rare variant possessing high levels of rare alleles, which is consistent with the fact that spontaneous cell fusion in animal cells is a rare event.

Partial Mitochondrial Genome Sequencing

The ovine mitochondrial *Cytb* gene and a fragment of the ovine mitogenome containing the control region have been used to haplotype sheep breeds and to study genetic diversity among and between sheep breeds [20,21,40]. In this study, we partially sequenced the *Cytb* gene and the mitochondrial fragment containing the control region and the *tRNA-Phe* and *12S rRNA* genes of the heart cell line to explore whether the spontaneous cell fusion led to mutational events in the mitogenome of the progeny cells. PSA of the partial sequences of the cell line at passages 26 and 59 revealed 54 gaps caused by an insertion of 35 bp in the 5' end and a deletion of 15 bp in the 3' end of the partial sequence of the *Cytb* gene in passage 59 cells. These insertion and deletion events in the *Cytb* gene of passage 59 cells might have caused changes in the genotype of *Cytb* gene SNPs as they were documented by the ovine bead chip genotyping of passage 47 cells of the FOH-SA cell line.

There was a similarity of 25.6% in the mitogenome segments spanning the control region and the *tRNA-Phe* and *12S rRNA* genes of the heart cell line at passages 26 and 59. The low similarity was caused by 583-bp gaps resulting from major deletion events in the segment of the mitogenome of passage 59 cells. The results of partial sequencing of the mitogenome of the heart cell line substantiated the results of SNP genotyping for the occurrence of large-scale genetic conversion in the progeny cells following spontaneous cell fusion. Osada et al [39] sequenced the complete mitogenome of the VERO cell line, and it was phylogenetically so diverse from *Chlorocebus sabaues* (the species from which it was established) that the VERO cell line could be clustered as a separate species.

We believe that the events associated with FOH-SA cell line development and VERO cell line establishment were analogous, that is, both cell lines evolved by spontaneous cell fusion. This reality was ascertained by several findings. First, a 3-hour culture of FOH-SA cells and that of VERO cells looked morphologically identical, with both showing an endothelial-like morphology (Figure S6 in Multimedia Appendix 1). Second, the endothelial-like morphology of the 3-hour culture of both cell lines was because both cell lines consisted of 2 cell types. One type descended from fibroblast-like cells usually showing rudimentary projections a few hours after incubation that soon disappeared with growth, and the other type descended from epithelial-like cells with morphological features indicative of the ancestors of the 2 cell lines. A comparison of the 3-hour

culture of VERO cells with heart cells at passage 22 (before transformation) strikingly demonstrated this fact (Figure S7 in [Multimedia Appendix 1](#)). Third, large-scale genetic conversion in both cell lines resulted in high levels of homozygosity in both cell lines, which could only be ascribed to spontaneous cell fusion. Fourth, major mutational events were detected in the mitogenomes of both cell lines. Future comparative studies of the mitogenomes of the FOH-SA and VERO cell lines will confirm the existence in the animal body of cell phenotypes that could spontaneously fuse and give rise to progeny cells that are genetically highly divergent from the parent cells.

Susceptibility of the Cell Line to Viruses

The cell line was found to be highly permissive to the RVF, PPR, LSD, camel pox, and sheep pox viruses; hence, it could be used for the isolation of these viruses as well as the development and production of vaccines. Cell immortalization was found to be associated with silencing or deletion of the IFN gene cluster [12], and the sensitivity of VERO cells to numerous viruses was also ascribed to the deletion of the IFN gene cluster [39]. Similarly, the sensitivity of FOH-SA cells to these viruses might be attributed to the deletion of the IFN gene cluster. A future genome landscape assessment of the cell line is expected to disclose this fact. SARS-CoV-2 and SAR-CoV-1 use angiotensin-converting enzyme 2 (ACE2) as a receptor for cell entry, and the ACE2 receptor is abundantly expressed on

cardiocytes, cardiofibroblasts, and coronary endothelial cells [41,42]. Hence, the FOH-SA cell line derived from heart tissue would be a good candidate for the propagation of SARS-CoV-2 and SARS-CoV-1 viruses.

Extended Incubation at 37 °C

A unique property of the FOH-SA cell line was the possibility of storing cultured cells at 37 °C for months provided that the growth medium was changed every 3 weeks. This property could be exploited as a short storage mechanism to avoid the cumbersome and risky cryopreservation of cells when they are needed within months, and this property could be useful in the propagation of slow-growing viruses. Shipment of this cell line could be done using cultures, which is more practical and economical than shipping on dry ice or liquid nitrogen. The capacity of FOH-SA cells stored at 37 °C to revert to multicellular filamentous growth similar to the filamentous growth documented in passages 29 to 32 is an important differentiating characteristic of this cell line.

Future studies on the FOH-SA cell line should investigate the molecular mechanisms of spontaneous cell fusion, the genome landscape of the cell line, the mitochondrial genome sequences of the cell line, the genes and pathways involved in immortalization, and the safety of the cell line in vaccine production, especially at high passages.

Acknowledgments

We would like to acknowledge Mohamed M Alfuhaid, who is the Director General of the General Administration of Laboratories, for his continuous support, encouragement, and enthusiasm. We greatly appreciate the close follow-up and the unlimited support of Dr Khaled S Abuhimed, Director of the Veterinary Vaccine Production and Evaluation Centre. We also greatly appreciate the help of Dr Hussain Al-Ghadeer and Dr Elgazali Guma, Veterinary Diagnostic Laboratory, Ministry of Environment, Water and Agriculture, Riyadh, in preparing DNA samples.

Data Availability

The partial sequence of the *cytochrome b* gene of the fetal ovine heart–Saudi Arabia (FOH-SA) cell line at passage 59 was submitted to NCBI GenBank and is available under accession number ON811684. The cell line at passage 51 was deposited at the American Type Culture Collection under the Budapest Treaty under patent accession number 125751 for availability.

Authors' Contributions

KS designed the study, performed the investigation, and analyzed the results. KS prepared the manuscript and revised it. MA participated in the preparation of the primary cell culture, passaging, and cryopreservation. GH collaborated in preparing the primary cell culture and testing the sensitivity of the cell line to viruses. HA participated in designing the study and supervised it.

Conflicts of Interest

None declared.

Multimedia Appendix 1

Supplementary findings.

[\[PDF File \(Adobe PDF File\), 1109 KB-Multimedia Appendix 1\]](#)

References

1. Eibl R, Eibl D, Pörtner R, Catapano G, Czermak P. Cell and Tissue Reaction Engineering. Berlin, Heidelberg. Springer; 2009.
2. Swain P. Basic techniques and limitations in establishing cell culture: a mini review. *Adv Anim Vet Sci*. 2014;2(4S):1-10. [doi: [10.14737/journal.aavs/2014/2.4s.1.10](https://doi.org/10.14737/journal.aavs/2014/2.4s.1.10)]

3. Verma A, Verma M, Singh A. Animal tissue culture principles and applications. In: Animal Biotechnology. Cambridge, MA. Academic Press; 2020:269-293.
4. Assanga I. Cell growth curves for different cell lines and their relationship with biological activities. *Int J Biotechnol Mol Biol Res*. Aug 31, 2013;4(4):60-70. [doi: [10.5897/ijbmr2013.0154](https://doi.org/10.5897/ijbmr2013.0154)]
5. Suleiman K, Boehnel H, Babiker S, Zaki A. Cytotoxic activity in fermenter culture supernatants of *Corynebacterium pseudotuberculosis*. *J Anim Vet Ad*. 2006;5:939-942. [FREE Full text]
6. Soice E, Johnston J. Immortalizing cells for human consumption. *Int J Mol Sci*. Oct 28, 2021;22(21):11660. [FREE Full text] [doi: [10.3390/ijms222111660](https://doi.org/10.3390/ijms222111660)] [Medline: [34769088](https://pubmed.ncbi.nlm.nih.gov/34769088/)]
7. Hayflick L, Moorhead P. The serial cultivation of human diploid cell strains. *Exp Cell Res*. 1961;25(3):585-621. [doi: [10.1016/0014-4827\(61\)90192-6](https://doi.org/10.1016/0014-4827(61)90192-6)]
8. Hayflick L. The cell biology of aging. *J Invest Dermatol*. Jul 1979;73(1):8-14. [FREE Full text] [doi: [10.1111/1523-1747.ep12532752](https://doi.org/10.1111/1523-1747.ep12532752)] [Medline: [448179](https://pubmed.ncbi.nlm.nih.gov/448179/)]
9. Kuilman T, Michaloglou C, Mooi WJ, Peeper DS. The essence of senescence. *Genes Dev*. Nov 15, 2010;24(22):2463-2479. [FREE Full text] [doi: [10.1101/gad.1971610](https://doi.org/10.1101/gad.1971610)] [Medline: [21078816](https://pubmed.ncbi.nlm.nih.gov/21078816/)]
10. Alessio N, Squillaro T, Cipollaro M, Bagella L, Giordano A, Galderisi U. The BRG1 ATPase of chromatin remodeling complexes is involved in modulation of mesenchymal stem cell senescence through RB-P53 pathways. *Oncogene*. Oct 07, 2010;29(40):5452-5463. [doi: [10.1038/onc.2010.285](https://doi.org/10.1038/onc.2010.285)] [Medline: [20697355](https://pubmed.ncbi.nlm.nih.gov/20697355/)]
11. Kumari R, Jat P. Mechanisms of cellular senescence: cell cycle arrest and senescence associated secretory phenotype. *Front Cell Dev Biol*. Mar 29, 2021;9:645593. [FREE Full text] [doi: [10.3389/fcell.2021.645593](https://doi.org/10.3389/fcell.2021.645593)] [Medline: [33855023](https://pubmed.ncbi.nlm.nih.gov/33855023/)]
12. Fridman AL, Tainsky MA. Critical pathways in cellular senescence and immortalization revealed by gene expression profiling. *Oncogene*. Oct 09, 2008;27(46):5975-5987. [FREE Full text] [doi: [10.1038/onc.2008.213](https://doi.org/10.1038/onc.2008.213)] [Medline: [18711403](https://pubmed.ncbi.nlm.nih.gov/18711403/)]
13. Shay JW, Wright WE. Telomeres and telomerase: three decades of progress. *Nat Rev Genet*. May 13, 2019;20(5):299-309. [doi: [10.1038/s41576-019-0099-1](https://doi.org/10.1038/s41576-019-0099-1)] [Medline: [30760854](https://pubmed.ncbi.nlm.nih.gov/30760854/)]
14. Madin SH, Darby NB. Established kidney cell lines of normal adult bovine and ovine origin. *Experimental Biology and Medicine*. Jul 01, 1958;98(3):574-576. [doi: [10.3181/00379727-98-24111](https://doi.org/10.3181/00379727-98-24111)]
15. Matsuura K, Inoshima Y, Kameyama K, Murakami K. Establishment of a novel ovine kidney cell line for isolation and propagation of viruses infecting domestic cloven-hoofed animal species. *In Vitro Cell Dev Biol Anim*. Aug 22, 2011;47(7):459-463. [FREE Full text] [doi: [10.1007/s11626-011-9434-3](https://doi.org/10.1007/s11626-011-9434-3)] [Medline: [21695582](https://pubmed.ncbi.nlm.nih.gov/21695582/)]
16. Sheets R. History and characterization of the Vero cell line. A report prepared by CDR Rebecca Sheets, Ph.D., USPHS. CBER/OVRR/DVRPA/VVB for the Vaccines and Related Biological Products Advisory Committee Meeting to be held on May 12, 2000. ResearchGate. URL: https://www.researchgate.net/profile/Awatif_Issa/post/Does_Vero_cell_possess_Fc_receptor_attachment/59d635e479197b80779935f0/AS:386030961217536%401469048361106/download/Verocell.pdf [accessed 2024-06-27]
17. Davis JM. Basic Cell Culture: A Practical Approach. Oxford, England. Oxford University Press; 1994.
18. Hebert PDN, Cywinska A, Ball SL, deWaard JR. Biological identifications through DNA barcodes. *Proc Biol Sci*. Feb 07, 2003;270(1512):313-321. [FREE Full text] [doi: [10.1098/rspb.2002.2218](https://doi.org/10.1098/rspb.2002.2218)] [Medline: [12614582](https://pubmed.ncbi.nlm.nih.gov/12614582/)]
19. Meadows J, Li K, Kantanen J, Tapio M, Sipos W, Pardeshi V, et al. Mitochondrial sequence reveals high levels of gene flow between breeds of domestic sheep from Asia and Europe. *J Hered*. 2005;96(5):494-501. [doi: [10.1093/jhered/esi100](https://doi.org/10.1093/jhered/esi100)] [Medline: [16135704](https://pubmed.ncbi.nlm.nih.gov/16135704/)]
20. Hiendleder S, Lewalski H, Wassmuth R, Janke A. The complete mitochondrial DNA sequence of the domestic sheep (*Ovis aries*) and comparison with the other major ovine haplotype. *J Mol Evol*. Oct 1998;47(4):441-448. [doi: [10.1007/pl00006401](https://doi.org/10.1007/pl00006401)] [Medline: [9767689](https://pubmed.ncbi.nlm.nih.gov/9767689/)]
21. Kärber G. Beitrag zur kollektiven Behandlung pharmakologischer Reihenversuche. *Archiv f experiment Pathol u Pharmakol*. Jul 1931;162(4):480-483. [doi: [10.1007/bf01863914](https://doi.org/10.1007/bf01863914)]
22. OvineSNP50 Genotyping BeadChip. Illumina. URL: https://www.illumina.com/documents/products/datasheets/datasheet_ovinesnp50.pdf [accessed 2024-06-27]
23. Madeira F, Pearce M, Tivey A, Basutkar P, Lee J, Edbali O, et al. Search and sequence analysis tools services from EMBL-EBI in 2022. *Nucleic Acids Res*. Jul 05, 2022;50(W1):W276-W279. [FREE Full text] [doi: [10.1093/nar/gkac240](https://doi.org/10.1093/nar/gkac240)] [Medline: [35412617](https://pubmed.ncbi.nlm.nih.gov/35412617/)]
24. National Committee of BioEthics Implementing Regulations of the Law of Ethics of Research on Living Creatures. National Committee of BioEthics. 2022. URL: <https://tinyurl.com/bye2xwef> [accessed 2024-06-27]
25. Shay J, Wright W. Senescence and immortalization: role of telomeres and telomerase. *Carcinogenesis*. May 2005;26(5):867-874. [doi: [10.1093/carcin/bgh296](https://doi.org/10.1093/carcin/bgh296)] [Medline: [15471900](https://pubmed.ncbi.nlm.nih.gov/15471900/)]
26. Lundberg AS, Hahn WC, Gupta P, Weinberg RA. Genes involved in senescence and immortalization. *Curr Opin Cell Biol*. Dec 2000;12(6):705-709. [doi: [10.1016/s0955-0674\(00\)00155-1](https://doi.org/10.1016/s0955-0674(00)00155-1)] [Medline: [11063935](https://pubmed.ncbi.nlm.nih.gov/11063935/)]
27. Smeets SJ, van der Plas M, Schaaïj-Visser T, van Veen EA, van Meerloo J, Braakhuis BJ, et al. Immortalization of oral keratinocytes by functional inactivation of the p53 and pRb pathways. *Int J Cancer*. Apr 01, 2011;128(7):1596-1605. [doi: [10.1002/ijc.25474](https://doi.org/10.1002/ijc.25474)] [Medline: [20499310](https://pubmed.ncbi.nlm.nih.gov/20499310/)]

28. Ogle BM, Cascalho M, Platt JL. Biological implications of cell fusion. *Nat Rev Mol Cell Biol.* Jul 15, 2005;6(7):567-575. [doi: [10.1038/nrm1678](https://doi.org/10.1038/nrm1678)] [Medline: [15957005](https://pubmed.ncbi.nlm.nih.gov/15957005/)]
29. Zhang H, Ma H, Yang X, Fan L, Tian S, Niu R, et al. Cell fusion-related proteins and signaling pathways, and their roles in the development and progression of cancer. *Front Cell Dev Biol.* Feb 1, 2021;9:809668. [FREE Full text] [doi: [10.3389/fcell.2021.809668](https://doi.org/10.3389/fcell.2021.809668)] [Medline: [35178400](https://pubmed.ncbi.nlm.nih.gov/35178400/)]
30. Alvarez-Dolado M. Cell fusion: biological perspectives and potential for regenerative medicine. *Front Biosci.* Jan 01, 2007;12(1):1-12. [doi: [10.2741/2044](https://doi.org/10.2741/2044)] [Medline: [17127279](https://pubmed.ncbi.nlm.nih.gov/17127279/)]
31. Bi P, Ramirez-Martinez A, Li H, Cannavino J, McAnally JR, Shelton JM, et al. Control of muscle formation by the fusogenic micropeptide myomixer. *Science.* Apr 21, 2017;356(6335):323-327. [FREE Full text] [doi: [10.1126/science.aam9361](https://doi.org/10.1126/science.aam9361)] [Medline: [28386024](https://pubmed.ncbi.nlm.nih.gov/28386024/)]
32. Pedrazzoli F, Chrysantzas I, Dezzani L, Rosti V, Vincitorio M, Sitar G. Cell fusion in tumor progression: the isolation of cell fusion products by physical methods. *Cancer Cell Int.* Sep 20, 2011;11(1):32. [FREE Full text] [doi: [10.1186/1475-2867-11-32](https://doi.org/10.1186/1475-2867-11-32)] [Medline: [21933375](https://pubmed.ncbi.nlm.nih.gov/21933375/)]
33. Kandušer M, Ušaj M. Cell electrofusion: past and future perspectives for antibody production and cancer cell vaccines. *Expert Opin Drug Deliv.* Dec 10, 2014;11(12):1885-1898. [doi: [10.1517/17425247.2014.938632](https://doi.org/10.1517/17425247.2014.938632)] [Medline: [25010248](https://pubmed.ncbi.nlm.nih.gov/25010248/)]
34. Ramos C, Teissié J. Electrofusion: a biophysical modification of cell membrane and a mechanism in exocytosis. *Biochimie.* May 2000;82(5):511-518. [doi: [10.1016/s0300-9084\(00\)00200-5](https://doi.org/10.1016/s0300-9084(00)00200-5)] [Medline: [10865136](https://pubmed.ncbi.nlm.nih.gov/10865136/)]
35. Littlefield JW. election of hybrids from mating of fibroblasts in vitro and their presumed recombinants. *Science.* Aug 14, 1964;145(3633):709-710. [doi: [10.1126/science.145.3633.709](https://doi.org/10.1126/science.145.3633.709)] [Medline: [14168277](https://pubmed.ncbi.nlm.nih.gov/14168277/)]
36. Sandenbergh L, Cloete S, Roodt-Wilding R, Snyman M, Bester-van der Merwe A. Evaluation of the OvineSNP50 chip for use in four South African sheep breeds. *SA J. An. Sci.* Apr 05, 2016;46(1):89. [doi: [10.4314/sajas.v46i1.11](https://doi.org/10.4314/sajas.v46i1.11)]
37. Ilori B, Rosen B, Sonstegard T, Bankole O, Durosaro S, Hanotte O. Assessment of OvineSNP50 in Nigerian and Kenyan sheep populations. *Nigerian J Biotechnol.* Mar 25, 2019;35(2):176. [doi: [10.4314/njb.v35i2.21](https://doi.org/10.4314/njb.v35i2.21)]
38. Cao Y, Song X, Shan H, Jiang J, Xiong P, Wu J, et al. Genome-wide association study of body weights in hu sheep and population verification of related single-nucleotide polymorphisms. *Front Genet.* Jul 3, 2020;11:588. [FREE Full text] [doi: [10.3389/fgene.2020.00588](https://doi.org/10.3389/fgene.2020.00588)] [Medline: [32719712](https://pubmed.ncbi.nlm.nih.gov/32719712/)]
39. Osada N, Kohara A, Yamaji T, Hirayama N, Kasai F, Sekizuka T, et al. The genome landscape of the african green monkey kidney-derived vero cell line. *DNA Res.* Dec 2014;21(6):673-683. [FREE Full text] [doi: [10.1093/dnares/dsu029](https://doi.org/10.1093/dnares/dsu029)] [Medline: [25267831](https://pubmed.ncbi.nlm.nih.gov/25267831/)]
40. Othman O, Germot A, Khodary M, Petit D, Maftah A. Cytochrome b diversity and phylogeny of six Egyptian sheep breeds. *Annu Res Rev Biol.* Jan 18, 2018;22(4):1-11. [doi: [10.9734/arrb/2018/38879](https://doi.org/10.9734/arrb/2018/38879)]
41. Tai W, He L, Zhang X, Pu J, Voronin D, Jiang S, et al. Characterization of the receptor-binding domain (RBD) of 2019 novel coronavirus: implication for development of RBD protein as a viral attachment inhibitor and vaccine. *Cell Mol Immunol.* Jun 2020;17(6):613-620. [FREE Full text] [doi: [10.1038/s41423-020-0400-4](https://doi.org/10.1038/s41423-020-0400-4)] [Medline: [32203189](https://pubmed.ncbi.nlm.nih.gov/32203189/)]
42. Patel VB, Zhong J, Grant MB, Oudit GY. Role of the ACE2/angiotensin 1–7 axis of the renin–angiotensin system in heart failure. *Circ Res.* Apr 15, 2016;118(8):1313-1326. [doi: [10.1161/circresaha.116.307708](https://doi.org/10.1161/circresaha.116.307708)]

Abbreviations

- ACE2:** angiotensin-converting enzyme 2
- ATCC:** American Type Culture Collection
- CPE:** cytopathic effect
- ECACC:** European Collection of Authenticated Cell Culture
- FADDL:** Foreign Animal Disease Diagnostic Laboratory
- FOH-SA:** fetal ovine heart–Saudi Arabia
- IFN:** interferon
- LSD:** lumpy skin disease
- MAF:** minor allele frequency
- MEM:** Minimum Essential Medium
- MEWA:** Ministry of Environment, Water and Agriculture
- MOI:** multiplicity of infection
- NCBE:** National Committee of Bioethics
- PCR:** polymerase chain reaction
- PPR:** Peste des petits ruminants
- PSA:** pairwise sequence alignment
- RVF:** Rift Valley fever
- SNP:** single nucleotide polymorphism
- TCID₅₀:** tissue culture infective dose 50
- USDA:** United States Department of Agriculture

Edited by T Leung, G Eysenbach; submitted 17.10.23; peer-reviewed by R Pillai, S Chakraborty, H Rafi, A Mukherjee; comments to author 22.03.24; revised version received 11.04.24; accepted 29.05.24; published 18.07.24

Please cite as:

Suleiman K, Aljulidan M, Hussein G, Alkhalaf H

Establishment of a Novel Fetal Ovine Heart Cell Line by Spontaneous Cell Fusion: Experimental Study

JMIRx Bio 2024;2:e53721

URL: <https://bio.jmirx.org/2024/1/e53721>

doi: [10.2196/53721](https://doi.org/10.2196/53721)

PMID:

©Khalid Suleiman, Mutaib Aljulidan, Gamaleldin Hussein, Habib Alkhalaf. Originally published in JMIRx Bio (<https://bio.jmirx.org>), 18.07.2024. This is an open-access article distributed under the terms of the Creative Commons Attribution License (<https://creativecommons.org/licenses/by/4.0/>), which permits unrestricted use, distribution, and reproduction in any medium, provided the original work, first published in JMIRx Bio, is properly cited. The complete bibliographic information, a link to the original publication on <https://bio.jmirx.org/>, as well as this copyright and license information must be included.